Specific Ion Adsorption at Hydrophobic Solid Surfaces

Dominik Horinek and Roland R. Netz

Physik Department, Technische Universität München, 85748 Garching, Germany

(Received 11 July 2007; published 29 November 2007)

Molecular dynamics simulations of ions at a hydrophobic self-assembled monolayer with polarizable force fields for water and ions are used to extract potentials of mean force for Na^+ and the halide ions Cl^-, Br^-, and I^-. Similar to the air-water interface, the large halide ions are attracted to the surface, which is traced back to surface-modified ion hydration. The total effective interaction is parametrized and used within Poisson-Boltzmann theory to calculate surface potentials and interfacial tensions at finite ion concentration in qualitative agreement with experiments.

DOI: 10.1103/PhysRevLett.99.226104 PACS numbers: 68.08.−p, 68.03.Cd, 82.45.Gj, 82.70.Uv

After more than 100 years, Hofmeister's observation that effective interactions between most charged and neutral objects in aqueous media depend crucially not only on electrolyte concentration but also on ion type has moved into the focus of current research again [1]. Ion specificity is most drastically revealed at uncharged hydrophobic solid surfaces and at the air-water interface: according to simple-minded theory, according to which ions are pointlike and interact solely via Coulomb forces, cations and anions should be equally repelled from such interfaces due to image-charge effects, leading to ion depletion at the surface, vanishing surface potentials, and a universal increase of surface tension [2]. Experimentally, on the other hand, it is found that for the free air-water interface (i) the surface-tension increment depends sensitively on the ion type [3], (ii) the surface potential for certain salts reaches values of up to 100 mV relative to pure water at molar concentration [3], and (iii) a negative charge is present at the interface, as inferred from thin-film stability and bubble electrophoresis [4,5]. Likewise, on solid hydrophobic surfaces the zeta potential is strongly negative and depends on ion type and concentration [6]; the presence of charges at the interface is confirmed by atomic force microscopy measurements using colloidal probes [7] and single polymers [8]. These interfacial ion-specific phenomena have a bulk counterpart: osmotic and activity coefficients also depend on the ion-type [9]. In fact, correlations between bulk and surface data suggest some underlying, not yet understood, microscopic relation [10].

Early on, theoretical models of surfaces were augmented to allow for generic short-ranged interactions between ions and surfaces [11]. These interactions were associated with dispersion forces or surface-modified ion hydration [4,12–14]. On the quantum-chemistry level, the adsorption energy of OH^- at self-assembled monolayers (SAMs) has been determined and shown to correlate well with experimental trends [15]. Unfortunately, such *ab initio* calculations can presently not be extended to finite temperatures. To yield microscopic insight including thermal effects, molecular dynamics (MD) simulations were used to obtain the effective interaction between ions and hydrophobic surfaces [16]. In MD, water, surface, and ion interactions are described by heuristic parameters (partial charges q and Lennard-Jones interaction range σ and depth ε_{LJ}) that are fitted to match experimental bulk data. As a major breakthrough, the adsorption of weakly hydrated ions (so-called chaotropic or structure breaking ions such as iodide or bromide) at the air-water interface was correctly obtained once the ionic polarizability α is included [17,18]. Although understanding the hydrophobic solid-water interface is important since it governs the aggregation and folding of unpolar molecules in water, previous simulations have concentrated on the air-water interface, mainly because more experimental reference data exist for it.

In this Letter we obtain the potential of mean force (PMF) for the halide anions and for sodium at infinite dilution at a hydrophobic SAM using MD simulations with polarizable force fields. The observed trend is similar to previous simulations at the air-water interface [17,18]: Heavy halide ions (Br^- and I^-) do adsorb, whereas the small cation Na^+ is repelled from the surface. The PMF includes image-charge effects, van der Waals interactions among ion, water, and substrate (as parametrized by ε_{LJ} and σ) and ion hydration. Surprisingly, the total van der Waals force is repulsive, so we conclude that the adsorption of large ions is mostly caused by surface-modified ion hydration. This might be a hint as to why hydrophobic surfaces and the air-water interface act alike when it comes to ion specificity (hence explaining the universality of the Hofmeister series [1]). Since no convincing, simple theory exists for the surface-modified ion hydration, a splitting of the PMF into physically motivated, analytic terms is pointless. We determine heuristic fit functions for the PMFs, which are used within a modified Poisson-Boltzmann approach to calculate ion distributions at finite ion concentration and from that the interfacial tension and electrostatic surface potential, showing qualitative agreement with experiments.

In the simulations, the hydrophobic surface is a 3 nm × 3.46 nm SAM consisting of 48 $C_{20}H_{42}$ chains that are terminally fixed with a grafting density appropriate for a

TABLE I. Force field parameters σ, ε_{LJ}, α, q in the MD simulations and the number of displaced water molecules n_W.

		σ [Å]	ε_{LJ} [kcal/mol]	$\alpha/4\pi\varepsilon_0$ [Å^3]	q [e]	n_W
Ions	Na^+	2.27	0.100	0.240	1	0.8
	Cl^-	4.34	0.100	4.0	−1	2.3
	Br^-	4.54	0.100	4.770	−1	2.4
	I^-	5.12	0.100	6.920	−1	2.8
Water	O	3.20	0.156	0.528	−0.730	
	H	0	0	0.170	0.365	
SAM	C	3.40	0.1094	0	AM1	
	H	2.64	0.0157	0	AM1	

gold substrate and assume the experimentally known 30° tilt angle [7]. The SAM is modeled with the gaff force field with AM1 charges [19]. The polarizabilities of the SAM atoms are small because of the SAM's low dielectric constant and are neglected in our simulations. The simulation box has an extension of 9 nm in the z direction and is filled with about 2,000 polarizable POL3 [20] water molecules. All force field parameters are listed in Table I. The simulations are done using the AMBER MD program [21] at a temperature of 300 K and pressure of 1 bar, maintained by anisotropic pressure coupling. Periodic boundary conditions are applied, and long-range Coulomb forces are calculated using particle-mesh Ewald summation. Figure 1 shows the water and SAM density profiles and the electrostatic potential along the z coordinate normal to the interface without ions. We observe a 0.15 nm thick water depletion layer [16] and an electrostatic potential drop of ~500 mV, in agreement with previous studies [22]. Next we place a single halide or sodium ion into the water phase and calculate its PMF by umbrella sampling and the weighted histogram analysis method [23]. We use previously optimized polarizable ion parameters [24] which correctly describe ion adsorption at the air-water interface. For Cl^- we use a higher polarizability value of $\alpha/4\pi\varepsilon_0 = 4$ Å^3 (as compared to the original value of $\alpha/4\pi\varepsilon_0 = 3.69$ Å^3), as suggested based on a comparison of classical and quantum-chemical MD simulations [25].

Our ionic PMFs at the SAM-water interface (solid symbols) are compared with previous air-water-interface results [24] (open symbols) for the same ions in Fig. 2. Both sets exhibit striking similarities. The big halides Br^- and I^- are attracted to the interface with an adsorption strength of almost $3k_BT$. While I^- has a higher affinity for air than Br^-, their affinity for the SAM is nearly the same. The PMFs for Cl^- are qualitatively different: We attribute the larger attraction at the SAM to the higher polarizability used. The behavior of sodium is similar at both interfaces and exhibits no attraction. In general, the interaction range is larger at the air-water interface, probably due to the intrinsic air-water interfacial roughness.

We first check whether the PMFs can be split into a sum of physically inspired terms. We note that ionic PMFs are excess quantities which result from replacing a certain number of water molecules n_W by an ion. We estimate n_W from simulated ion-water radial-distribution functions in bulk; see Table I. Any charged object interacts with the substantial electrostatic interfacial water potential $\Phi_W(z)$, which is caused by preferential water orientation. Assuming the presence of the ion of charge q does not modify Φ_W, one obtains the interaction contribution $V^\Phi = q\Phi_W(z)$. We fit the potential $\Phi_W(z)$ by a sum of four tanh terms and a constant; the resulting fit is shown in Fig. 1 (solid line). The excess polarization energy of an ion in the water electric field $E_W(z) = -d\Phi_W(z)/dz$ is $V^{pol}(z) = -\frac{1}{2}(\alpha - n_W\alpha_W)E_W^2(z)$, where the polarization energy of n_W replaced water molecules with polarizability α_W is subtracted. The van der Waals (vdW) interaction of either an ion or a water molecule with the SAM is obtained at zero temperature performing a sum over all Lennard-Jones interactions between SAM sites and the particle with a cutoff radius of 9 Å and averaging over lateral positions. The obtained energy is fitted to a 9-6 Lennard-Jones potential $V^{vdW} = 4\bar{\varepsilon}_{LJ}\{[\bar{\sigma}/(z - z_0)]^9 - [\bar{\sigma}/(z - z_0)]^6\}$ with different parameters for every ion type and water. The excess potential is obtained as $\Delta V^{vdW} = V^{vdW} - n_W V_W^{vdW}$ by subtracting the vdW potential of n_W replaced water molecules. For the image-charge repulsion of the ions from the SAM we use a closed-form expression $V^{img}(z)$ for finite-size charged spheres [13]. For the sphere radius we take $\sigma/2$ as defined in Table I and $\varepsilon = 80$ and $\varepsilon = 1$ for the relative dielectric constants in the water and

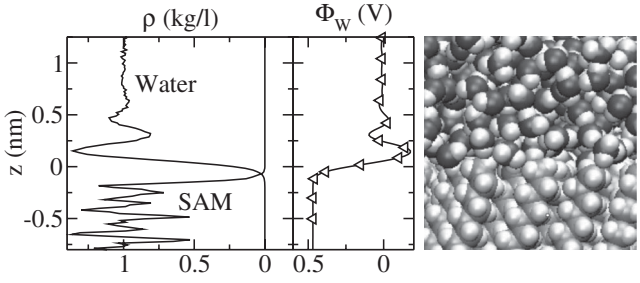

FIG. 1. Density profiles $\rho(z)$ of water and SAM and the electrostatic water potential Φ_W. Triangles show the simulated Φ_W; the line shows a heuristic fit function (see text). To the right: Snapshot of the SAM-water interface.

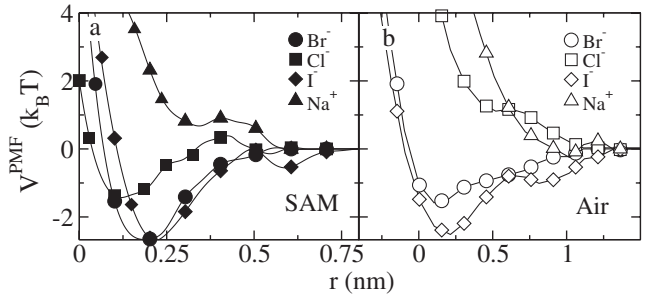

FIG. 2. Potentials of mean force for various ions at the (a) SAM-water and the (b) air-water [24] interface. The lines show heuristic fits with the parameters in Table II.

SAM half spaces. We approximate the total ionic PMF as the sum $V^{\mathrm{PMF}}(z) = V^{\Phi}(z) + \Delta V^{\mathrm{vdW}}(z) + V^{\mathrm{pol}}(z) + V^{\mathrm{img}}(z)$, which is shown for iodide in Fig. 3 (solid line) together with all four contributions. Comparison with the simulated PMF (triangles) gives poor agreement. In particular, the vdW part ΔV^{vdW} (dotted line) makes up for only a small fraction of the total ion-SAM attraction V^{PMF}. This is further enhanced by the fact that the vdW interaction between the ion and water is reduced as the ion approaches the surface and gives rise to a repulsive interaction which has been extracted from the simulation (circles); this makes the total vdW contribution to the PMF in fact *repulsive*. We conclude that the surface-induced modification of the ion hydration (which has been left out from our consideration as it is difficult to estimate) dominates the PMF. This is in line with our observation that PMFs at the interface toward a hydrophobic SAM and air are quite similar, showing that it is the water structure that is important and not so much the interaction of ions with the nonaqueous half-space. Still, the polarizability is essential as well. This is evident from our study of nonpolarizable ions at a hydrophobic diamond substrate [26], where we found negligible attraction. Instead of cooking up an expression for the distance-dependent ion hydration, we fit the whole PMF by a heuristic function. For the SAM data we use $V^{\mathrm{fit}}(z)/k_BT = A/(z-z')^{12} - B/(z-z')^8 + C_1(z-C_2)e^{-C_3(z-C_2)^2} + D_1 e^{-D_3(z-D_2)^2}$ and for the air-water interface data [24] we use $V^{\mathrm{fit}}(z)/k_BT = A\{[e^{-B(z-z')} + (-1)^n]^2 - 1\} + C_1(z-C_2)e^{-C_3(z-C_2)^2} + D_1 e^{-D_3(z-D_2)^2}$ with $n = 1$ for the attractive Br^- and I^-, and $n = 2$ for Cl^- and Na^+. All fit parameters are given in Table II; note that the distance z in the fit functions is rescaled by nm and is thus unitless. The fit functions are shown as solid lines in Fig. 2 along with the simulation data. We next demonstrate how PMFs can be used for a coarse-grained description of

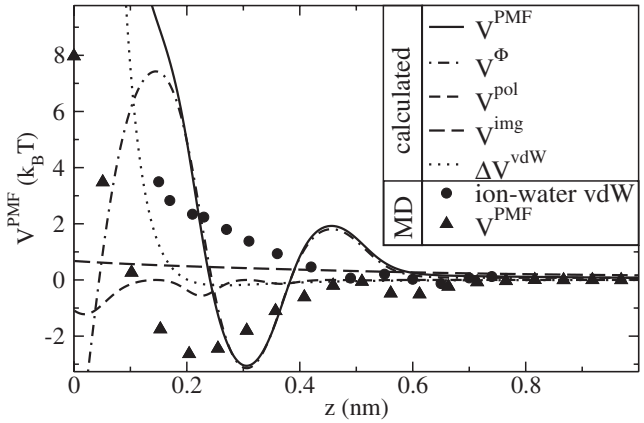

FIG. 3. Potential of mean force for iodide from simulation (triangles) compared with the analytic expression (solid line) and its contributions. Poor agreement shows that surface-modified ion hydration is dominant. The ion-water van der Waals contribution [as obtained from simulations (circles)] makes the total van der Waals interaction repulsive.

ion specificity at interfaces. For this we consider a modified Poisson-Boltzmann equation for unpolarizable particles [4,12,14]

$$\varepsilon \frac{d^2}{dz^2}\Phi(z) = -\sum_i q_i c_i^0 e^{-[V_i^{\mathrm{PMF}}(z) + q_i\Phi(z)]/k_BT},$$

where the PMF from our MD simulations V_i^{PMF} is included [27]. Note that Φ is the electrostatic potential without polarization contributions. The solution to the equation satisfies the boundary conditions that (i) $\Phi = 0$ in bulk water ($z \to \infty$) and (ii) $\Phi = \mathrm{const}$ for $z \to -\infty$. Figure 4(b) shows the rescaled ionic density profiles $c(z)/c^0$ for different bulk salt concentration c^0 both at the SAM and at the air-water interface (inset). Figure 4(a) shows the surface potential $\Delta\Phi$ at the SAM-water (solid symbols) and air-water (open symbols) interface as a function of electrolyte concentration. The effect of salt addition is similar at both interfaces and lowers $\Delta\Phi$. For NaCl at the air-water interface, the change is very small, since both ions are repelled from the surface. In all other cases, there is a significant drop of the surface potential, between -20 mV (NaCl at the SAM-water interface) and -58 mV (NaI at the air-water interface) for a 1 M electrolyte. Ignoring the behavior for small salt concentration at the moment, the slope of $\Delta\Phi(c^0)$ at $c^0 \simeq 1$ M agrees well with experimental data [3]: the experimental and predicted slopes in mV/M in the high concentration range at the air-water interface are $-20/-18$ (NaI), $-14/-15$ (NaBr), and $-8/-1$ (NaCl). Only for NaCl, there is a strong underestimation, which reflects the lack of Cl^- attraction in the PMF and might be due to a too small ionic polarizability.

We calculate the surface-tension change with salt concentration from the Gibbs adsorption equation

$$\Delta\gamma = -k_BT \int_0^{c^0} \sum_i \Gamma_i/c'dc',$$

where Γ_i denotes the surface excess of ionic species i, $\Gamma_i = \int_{-\infty}^{\mathrm{GDS}} c_i(z)dz + \int_{\mathrm{GDS}}^{\infty}[c_i(z) - c_i^0]dz$, and GDS is the position of the Gibbs-dividing surface. Figure 4(c) shows $\Delta\gamma$ for different ions at both interfaces. The interfacial tensions

TABLE II. Fit parameters of the fit functions for ionic PMFs at the SAM (upper set) and the air-water interface (bottom).

SAM	A	B	z'	C_1	C_2	C_3	D_1	D_2	D_3
I^-	50.73	18.99	−1.09	−10.22	0.54	200	−2.51	0.21	60.24
Br^-	0.51	0.92	−0.74	0	0	0	−2.33	0.18	46.41
Cl^-	1.20	−1.05	−0.99	−7.74	0.48	200	−2.26	0.12	60.61
Na^+	−2.22	−7.33	−0.89	10.28	0.37	100	−0.28	0.12	2.58
Air	A	B	z'	C_1	C_2	C_3	D_1	D_2	D_3
I^-	0.066	0.977	2.39	−5.1	0.70	8.7	−7.32	−0.011	2.49
Br^-	0.042	1.77	1.23	−5.0	0.40	10.0	−4.05	0.042	8.16
Cl^-	15.16	4.13	−0.37	0	0	0	0.68	0.70	23.99
Na^+	14.62	4.35	−0.084	4.13	1.10	50.0	−0.37	0.70	10.0

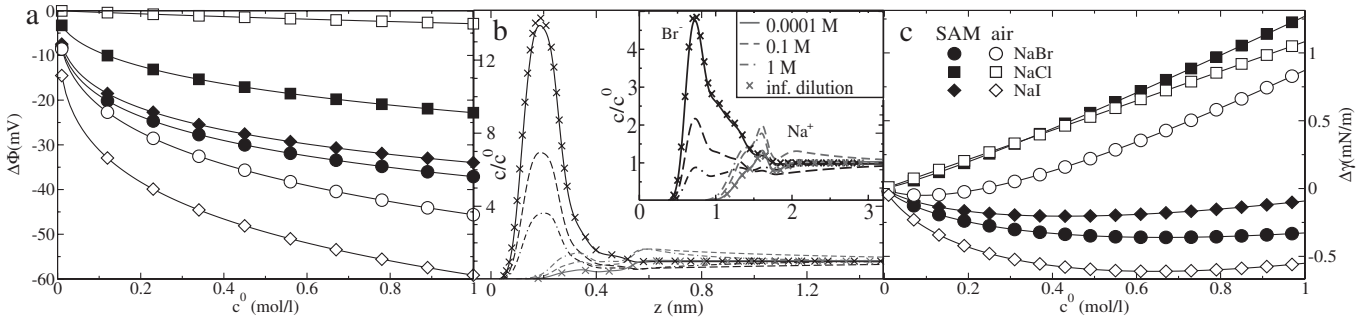

FIG. 4. (a) Surface potential $\Delta\Phi$ as a function of bulk salt concentration c^0 for various ions at the SAM-water interface (solid symbols) and the air-water interface (open symbols) as obtained from the ion density profiles in (b). (b) Rescaled cationic or anionic density profiles $c(z)/c^0$ of NaBr at the SAM-water interface and the air-water interface (inset) for infinite dilution (crosses) and different bulk concentrations c^0, as obtained by inserting the simulation PMFs into a Poisson-Boltzmann equation. (c) Surface-tension change as a function of c^0 for various ions as obtained from the Gibbs adsorption equation.

increase nearly linearly with the addition of NaCl, because the repulsion of Na^+ is stronger than the attraction of Cl^-. Experimentally, NaCl addition gives a linear increase of the air-water surface tension with a slope of 1.7 $mN\,m^{-1}/M$ [3], ~30% higher than we predict. An attractive PMF does not necessarily lead to a decrease of the surface tension: only for $c^0 \to 0$, $d\gamma/dc^0$ is negative for the strongly adsorbing bromide and iodide ions; for larger concentrations the slope changes due to ion-ion interactions which are taken into account by the Poisson-Boltzmann formalism. For larger concentration our results agree with the experimentally found linear increase of the interfacial tension for NaBr with a slope of 1.4 $mN\,m^{-1}/M$ [3] within ~30%. For NaI the experimental slope of 1.2 $mN\,m^{-1}/M$ is not reproduced by our calculations, which might signal a breakdown of our mean-field analysis or a maladjusted force field.

Combining MD simulations with continuum statistical mechanics approaches is introduced as a promising approach toward interfacial ion specificity. Interfacial tension and potential at the air-water interface agree qualitatively with experimental data and the Hofmeister series is reproduced: the heavier halides adsorb stronger and therefore the surface potential is more negative and the surface-tension increase is weaker. At the solid hydrophobic surface we obtain the same trends.

Discussions with W. Kunz, P. Jungwirth, B. Ninham, and M. Boström and financial support from the German Excellence Initiative via the Nanosystems Initiative Munich (NIM), the Elite Netzwerk Bayern (CompInt), and the Ministry for Economy and Technology (BMWi) in the framework of the AiF project "Simulation and Prediction of Salt Influence on Biological Systems" are acknowledged.

[1] W. Kunz, J. Henle, and B. W. Ninham, Curr. Opin. Colloid Interface Sci. **9**, 19 (2004).
[2] L. Onsager and N. N. T. Samaras, J. Chem. Phys. **2**, 528 (1934).
[3] N. L. Jarvis and M. A. Scheiman, J. Phys. Chem. **72**, 74 (1968).
[4] K. A. Karraker and C. J. Radke, Adv. Colloid Interface Sci. **96**, 231 (2002).
[5] K. Ciunel *et al.*, Langmuir **21**, 4790 (2005).
[6] R. Schweiss *et al.*, Langmuir **17**, 4304 (2001).
[7] K. Feldman *et al.*, J. Am. Chem. Soc. **121**, 10 134 (1999).
[8] C. Friedsam, H. Gaub, and R. R. Netz, Europhys. Lett. **72**, 844 (2005).
[9] W. Kunz *et al.*, J. Phys. Chem. B **108**, 2398 (2004).
[10] P. K. Weissenborn and R. J. Pugh, J. Colloid Interface Sci. **184**, 550 (1996).
[11] R. Podgornik, Chem. Phys. Lett. **156**, 71 (1989).
[12] M. Boström, D. R. M. Williams, and B. W. Ninham, Langmuir **17**, 4475 (2001).
[13] V. S. Markin and A. G. Volkov, J. Phys. Chem. B **106**, 11 810 (2002).
[14] M. Manciu and E. Ruckenstein, Adv. Colloid Interface Sci. **105**, 63 (2003).
[15] H. J. Kreuzer, R. L. C. Wang, and M. Grunze, J. Am. Chem. Soc. **125**, 8384 (2003).
[16] S.-J. Marrink and S. Marcelja, Langmuir **17**, 7929 (2001).
[17] P. Jungwirth and D. J. Tobias, Chem. Rev. **106**, 1259 (2006).
[18] T. M. Chang and L. X. Dang, Chem. Rev. **106**, 1305 (2006).
[19] J. M. Wang *et al.*, J. Mol. Graph. Mod. **25**, 247 (2006).
[20] J. W. Caldwell and P. A. Kollman, J. Phys. Chem. **99**, 6208 (1995).
[21] D. A. Pearlman *et al.*, Comput. Phys. Commun. **91**, 1 (1995).
[22] V. P. Sokhan and D. J. Tidesley, Mol. Phys. **92**, 625 (1997).
[23] S. Kumar *et al.*, J. Comput. Chem. **13**, 1011 (1992).
[24] L. X. Dang, J. Phys. Chem. B **106**, 10 388 (2002).
[25] P. Jungwirth and D. Tobias, J. Phys. Chem. A **106**, 379 (2002).
[26] P. Kölsch *et al.*, Colloids Surf. A **303**, 110 (2007).
[27] G. Luo *et al.*, Science **311**, 216 (2006).